CASAnova: a multiclass support vector machine model for the classification of human sperm motility patterns†

Summer G. Goodson[1], Sarah White[2], Alicia M. Stevans[3], Sanjana Bhat[3], Chia-Yu Kao[2], Scott Jaworski[1], Tamara R. Marlowe[1], Martin Kohlmeier[1,4], Leonard McMillan[2], Steven H. Zeisel[1,4,*] and Deborah A. O'Brien[3,*]

[1]University of North Carolina at Chapel Hill Nutrition Research Institute, Kannapolis, North Carolina, USA; [2]Department of Computer Science, University of North Carolina at Chapel Hill, Chapel Hill, North Carolina, USA; [3]Department of Cell Biology and Physiology, University of North Carolina at Chapel Hill School of Medicine, Chapel Hill, North Carolina, USA and [4]Department of Nutrition, University of North Carolina at Chapel Hill, Chapel Hill, North Carolina, USA

*__Correspondence:__ Steven H. Zeisel, University of North Carolina at Chapel Hill Nutrition Research Institute, 500 Laureate Way, Kannapolis, NC, 28081; Tel: 704-250-5000; E-mail: steven_zeisel@unc.edu; Deborah A. O'Brien, Department of Cell Biology and Physiology, CB#7545, 220 Taylor Hall, University of North Carolina School of Medicine, Chapel Hill, NC, 27599; Tel: 919-357-7564; E-mail: dao@med.unc.edu

†__Grant support:__ This work was supported by National Institutes of Health grant U01 HD060481 from the Eunice Kennedy Shriver National Institute of Child Health and Human Development and NIDDK grant P30DK056350 to the UNC Nutrition Obesity Research Center.

Received 6 March 2017; Revised 5 August 2017; Accepted 1 October 2017

Abstract

The ability to accurately monitor alterations in sperm motility is paramount to understanding multiple genetic and biochemical perturbations impacting normal fertilization. Computer-aided sperm analysis (CASA) of human sperm typically reports motile percentage and kinematic parameters at the population level, and uses kinematic gating methods to identify subpopulations such as progressive or hyperactivated sperm. The goal of this study was to develop an automated method that classifies all patterns of human sperm motility during in vitro capacitation following the removal of seminal plasma. We visually classified CASA tracks of 2817 sperm from 18 individuals and used a support vector machine-based decision tree to compute four hyperplanes that separate five classes based on their kinematic parameters. We then developed a web-based program, CASAnova, which applies these equations sequentially to assign a single classification to each motile sperm. Vigorous sperm are classified as progressive, intermediate, or hyperactivated, and nonvigorous sperm as slow or weakly motile. This program correctly classifies sperm motility into one of five classes with an overall accuracy of 89.9%. Application of CASAnova to capacitating sperm populations showed a shift from predominantly linear patterns of motility at initial time points to more vigorous patterns, including hyperactivated motility, as capacitation proceeds. Both intermediate and hyperactivated motility patterns were largely eliminated when sperm were incubated in noncapacitating medium, demonstrating the sensitivity of this method. The five CASAnova classifications are distinctive and reflect kinetic parameters of washed human sperm, providing an accurate, quantitative, and high-throughput method for monitoring alterations in motility.

Summary Sentence

A CASA-based support vector machine model of human sperm motility provides rapid, accurate, and quantitative analysis of all motile sperm in a population.

Key words: sperm motility, CASA, hyperactivation, capacitation, support vector machine, CASAnova.

Introduction

The utilization of computer-aided sperm analysis (CASA) to analyze sperm motility has proven successful in studies of sperm function in multiple species. CASA detects the position of sperm heads in multiple microscopic fields and uses algorithms to generate tracks monitoring sperm movement over a short interval, with kinematic parameters describing sperm velocities and proxy measurements for tail movement. Standard parameters include average path velocity (VAP), straight-line velocity (VSL), curvilinear velocity (VCL), amplitude of lateral head displacement (ALH), beat cross frequency (BCF), straightness (STR, VSL/VAP), and linearity (LIN, VSL/VCL). Population means or medians of these individual parameters have been used to monitor motility changes in response to certain treatments or genetic perturbations [1–3], but are not necessarily reflective of changes in physiologically important patterns of motility.

Gating methods that set threshold values for specific kinetic parameters are often used to classify subsets of sperm populations with distinct patterns of motility. Immediately after collection, sperm typically exhibit rapid, linear motility, producing CASA tracks that are predominantly classified as progressive based on thresholds for STR and VAP. Sperm with VAP $\geq$ 25 μm/s are considered rapid, based on earlier World Health Organization (WHO) recommendations for visually assessing motility in semen samples [4]. During capacitation in the female reproductive tract or in media mimicking the oviductal environment, a portion of the sperm population exhibits altered flagellar beating patterns to become hyperactivated [5]. This vigorous, less progressive form of motility may facilitate sperm transport in the oviduct and is thought to generate forces important for penetrating the zona pellucida [6]. Both the onset and maintenance of hyperactivation are critical, as genetic perturbations of these events are associated with infertility [7–10]. Clinical studies indicate that hyperactivation of human sperm is correlated with fertility [11–13] and that calcium signaling mediates this functional change in motility patterns [14, 15]. In CASA analyses, hyperactivated human sperm are identified by setting threshold gates for a combination of kinematic parameters [14, 16–22], most frequently VCL $\geq$ 150 μm/s, LIN $\leq$ 50%, and ALH $\geq$ 7 μm for sperm analyzed at 60 Hz [17].

Our CASA analyses of mouse sperm identified both vigorous and nonvigorous patterns of motility that developed during in vitro capacitation [23]. Therefore, we developed a new approach to rapidly classify each motile sperm within a population as progressive, intermediate, hyperactivated, slow, or weakly motile [23]. This method combines support vector machine (SVM) equations, a commonly used method of supervised machine learning, into a multiclass decision tree that uses all five independent kinematic parameters to classify the motility pattern of individual sperm [24]. CASAnova, the automated software version of this model, has proven useful for analyzing the effects of genetic and metabolic alterations on sperm motility [25–28]. For example, this method revealed distinct differences in sperm motility between founder strains and in extinct lines of the Collaborative Cross [29, 30]. It has been used to assess the impact of protectants on sperm hyperactivation following cryopreservation [31] and to monitor calcium ionophore stimulation of hyperactivation in sterile knockout models [32]. These studies demonstrate the power of identifying multiple patterns of sperm motility in a standardized way that can be compared across studies and between research groups.

To our knowledge, CASA guidelines have not been developed for classifying all motility patterns of human sperm after processing to remove seminal plasma. Only the gates for hyperactivated sperm were established using processed sperm samples since seminal plasma inhibits hyperactivation [17]. Since velocities and other CASA parameters increase significantly in processed human samples [33–35], "rapid" and other designations based on semen samples do not discriminate differences across the full range of kinetic parameters exhibited by washed sperm. Therefore, we adapted the CASAnova method for the analysis of human sperm after determining that human and mouse sperm undergo similar changes in vigorous and nonvigorous motility patterns during capacitation. This study describes the development of the human CASAnova model, assesses its performance under different conditions, and compares its results with current gating methods that define motility patterns for subsets within a sperm population.

Materials and methods

Study design and ethics

The design and procedures used in the study were approved by the University of North Carolina at Chapel Hill Institutional Review Board. All subjects were at least 18 years of age. Informed written consent was obtained from all subjects prior to collection of any material. Subjects were recruited from the greater Charlotte, NC area in response to mass emails, ads in print media, social media, and flyers advertising a separate study at the UNC Nutrition Research Institute in Kannapolis, NC.

Chemicals and reagents

ISolate Concentrate, human tubal fluid (HTF) medium and modified HTF (mHTF) medium were obtained from Irvine Scientific (Irvine, CA, USA). All other chemicals and reagents were obtained from Sigma-Aldrich (St. Louis, MO, USA) unless otherwise noted.

Sample collection and processing

Subjects were asked to refrain from sexual activity for 72 h prior to collection. Semen was collected by masturbation into sterile 50 ml sample cups. Samples were then incubated for 30 min at 37°C under 5% CO_2 in air to allow liquefaction. Semen volume was measured with a pipette, and the sample was then gently layered over 2 ml of ISolate diluted to 45% (v/v) with mHTF medium that had been pre-warmed at 37°C. The mHTF medium contains 101.6 mM NaCl, 4.7 mM KCl, 0.37 mM KH_2PO_4, 0.2 mM $MgSO_4{\cdot}7H_2O$, 2 mM $CaCl_2$, 21 mM HEPES, 4 mM sodium bicarbonate 2.78 mM glucose, 0.33 mM pyruvate, and 21.4 mM lactate and is supplemented with 5 mg/ml bovine serum albumin. This medium does not induce capacitation due to its reduced bicarbonate content [36, 37]. Samples were centrifuged at 300 × g for 20 min at 37°C. This single layer step gradient removes semen constituents and round cells

in the upper layer and collects sperm in the pellet [38, 39], enabling subsequent motility analysis of all sperm in the sample. The resulting sperm pellets were washed twice with 3 ml each mHTF followed by centrifugation at 300 × g for 10 min at 37°C. Sperm were then resuspended in 1 ml mHTF, and an aliquot was taken for determination of sperm count and concentration. All samples used in the training of the model exceeded lower reference limits for sperm count and motility according to the WHO guidelines [40].

Analysis of sperm motility

Washed sperm pellets were resuspended and diluted at least 1:20 (to reduce the likelihood of tracking errors due to high concentrations of sperm per field) in HTF complete medium (containing 25 mM sodium bicarbonate and no HEPES) and incubated at 37°C under 5% CO_2 in air, conditions which support sperm capacitation [41, 42]. Motility was assessed at 1-h intervals over a 5-h incubation period. Noncapacitating control samples were also diluted at least 1:20 in mHTF. Using a large-bore pipette tip, each sperm aliquot was loaded into a Microtool semen analysis slide with a depth of 20 μm (Cytonix, Beltsville, MD) and motility was analyzed using a Hamilton Thorne IVOS II Clinical Analysis System (Hamilton Thorne Biosciences, Beverly, MA). Human Motility II software (version 14.0) was used to record quantitative parameters of sperm motility, including Field #, Track #, VAP (μm/s), VSL (μm/s), VCL (μm/s), STR (VSL/VAP), LIN (VSL/VCL), ALH (μm), and BCF (Hz). One-second tracks were captured using the following settings: 60 frames per second, 60 frames acquired, minimum contrast = 80, minimum size = 3 pixels, default cell size = 6 pixels, default cell intensity = 160, slow cells counted as motile, low VAP cutoff = 10 μm/s, low VSL cutoff = 0 μm/s, minimum intensity gate = 0.18, maximum intensity gate = 1.21, minimum size gate = 0.56 pixels, maximum size gate = 2.63 pixels, minimum elongation gate = 0 pixels, and maximum elongation gate = 99 pixels. As recommended by the WHO guidelines for semen analysis [40], we recorded a total of ~200–400 sperm in 20 adjacent, nonoverlapping fields for each sample at each time point, and tracks containing less than 30 points were excluded from further analysis. The percentage of motile sperm in each population was determined, and kinematic parameters of each track at each time point were recorded in database text (DBT) files. Where appropriate, the SORT function was used to identify the number of tracks meeting kinematic threshold gates (VCL ≥ 150 μm/s, LIN ≤ 50%, ALH ≥ 7 μm) previously defined for hyperactivated tracks [17].

Human CASAnova model training

Time points from multiple samples were visually assessed to identify the intervals with the most diverse patterns of motility. As the 3-h time point displayed a good diversity of motility patterns, we used this time point to create the CASAnova training set, with all individual tracks scored by at least two trained observers. Since the observed motility patterns closely approximated those identified for mouse sperm, previously published criteria were used to classify individual tracks as progressive, intermediate, hyperactivated, slow, and weakly motile [23]. These criteria incorporated strict guidelines to distinguish these classes based on deviation from the average path, angles between adjacent points in the track, and the overall length of the track (details are provided in the Results section). We examined published examples of CASA tracks from human sperm identified as hyperactivated [16, 18, 34, 43, 44] to insure that our criteria were consistent with accepted standards for human hyperactivation. Consequently, all hyperactivated tracks included in the dataset exhibited angles >90° between consecutive points along the majority of the path. The corresponding kinematic parameters for each motility class were identified from DBT files and manually grouped according to their visual classification in a Microsoft Excel sheet to create a training set. These parameters and classifications were loaded into Matlab (version 2014b; The Mathworks), and the LIBSVM library was used to generate SVM equations that delineate motility groups using the same decision-tree topology employed for mouse sperm [23]. Each SVM equation was trained with the training set using a K-fold cross validation approach [45]. We determined the overall classification accuracy (true positives/n) and class-specific performance measures (precision, sensitivity, and specificity) using the multiclass confusion matrix approach [46].

Statistical analysis

Statistical analyses were performed using GraphPad Prism 6 (GraphPad Software, La Jolla, CA, USA). Most data are presented as mean values ± SEM. Medians and ranges for kinematic parameters are shown in Figure 3. Statistical significance between percentages was determined using two-tailed unpaired *t*-tests after arcsine transformation of percentages. For statistical analyses comparing methods for identifying hyperactivated sperm (Figure 7), statistical differences were determined with one-way ANOVA followed by Dunnett's post test for multiple comparisons. Differences were considered to be significant if $P < 0.05$.

Results

Classification of sperm motility

Analysis of CASA tracks for human sperm from 18 individuals showed changes in motility patterns during capacitation. Progressive linear motility was predominant at initial time points (Figure 1A), with the subsequent appearance of less linear patterns (Figure 1B). Since the track patterns observed during this incubation were very similar to the five motility groups initially reported for mouse sperm [23], we applied the same SVM approach to determine if we could develop a robust CASAnova model for the classification of human sperm motility patterns. We visually classified tracks from capacitating sperm incubated for 3 h in HTF medium to generate a training data set for this model, since this time point displayed good diversity in motility patterns. Each track was classified by at least two trained observers as progressive (Figure 2A), intermediate (Figure 2B), hyperactivated (Figure 2C–E), slow (Figure 2F), or weakly motile (Figure 2G) according to the strict criteria that evaluate track length, deviation from the average path, and angles between adjacent points in the track [23]. Sperm were identified as progressive if the tracks were generally straight with little deviation of the head from the average path of movement and angles <90° between consecutive points along the majority of the path. Intermediate sperm exhibited larger deviations from the average path of movement resulting in wider tracks, with angles between adjacent points of approximately 90° along most of the track. Tracks of hyperactivated sperm covered less forward distance relative to their vigor, displaying large deviations of the head from the path of movement and angles >90° between adjacent points. Slow sperm were similar to progressive sperm but traveled less distance, producing tracks that were generally 50% or less the length of progressive sperm tracks. Lastly, weakly motile sperm displayed sluggish movement with very

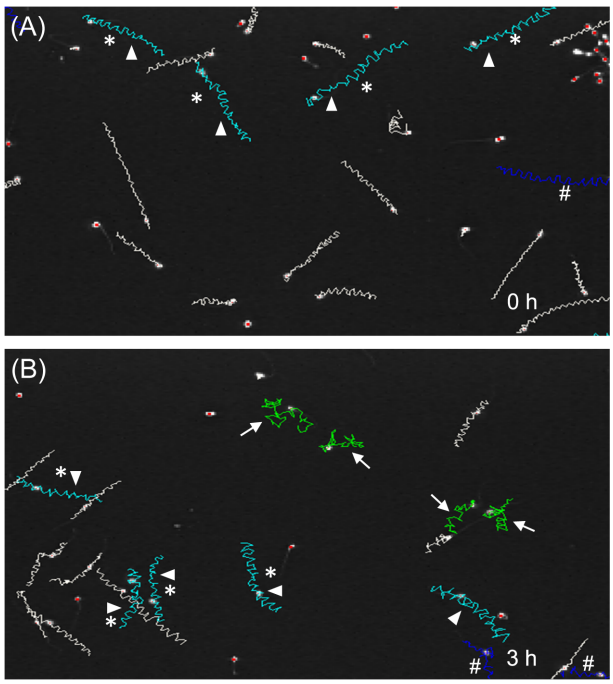

Figure 1. Time-dependent changes in sperm motility patterns during *in vitro* capacitation. Representative images from computer-aided sperm analysis (CASA) of human sperm from a single individual incubated for 0 h (A) or 3 h (B) in HTF complete medium. Gates corresponding to VCL $\geq$ 150 μm/s, LIN $\leq$ 50% and ALH $\geq$ 7 μm were applied to the sperm tracks using the CASA SORT function. These gates identifed both the cyan (arrow heads) and green tracks (arrows) as hyperactivated. The green tracks are also classified as non-progressive, based on CASA-dependent settings. Dark blue (#) tracks denote sperm that left the field before analysis was completed. Asterisks denote tracks that meet the criteria of the SORT function, but do not meet our strict criteria of hyperactivated sperm patterns by visual analysis.

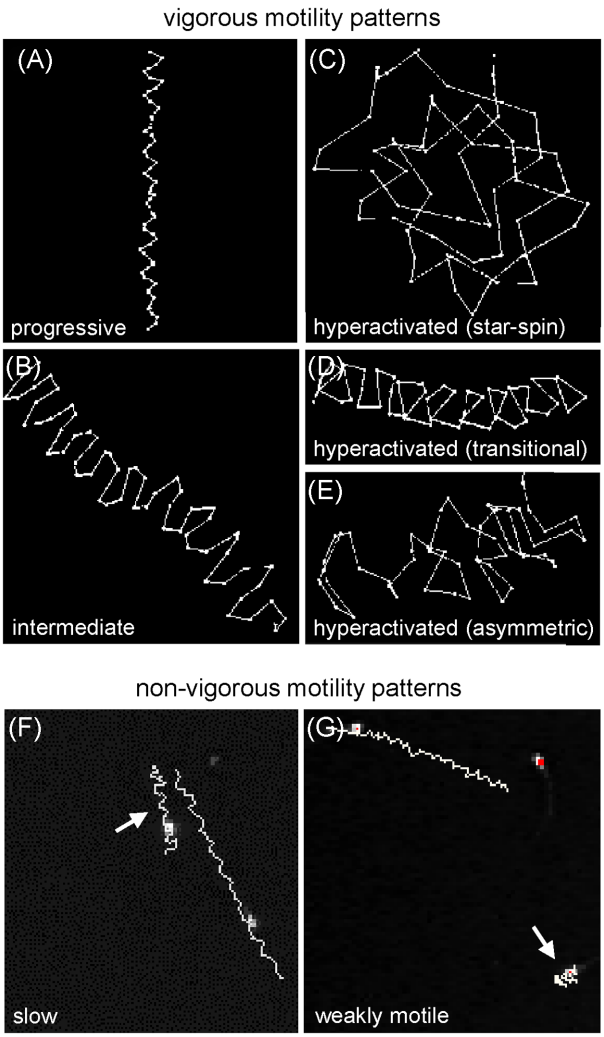

Figure 2. Examples of human sperm motility patterns identified during in vitro capacitation. Representative CASA tracks displaying vigorous motility patterns (A–E) after 3 h in capacitating medium were visually classified as progressive (A), intermediate (B), or hyperactivated (C–E).Vigorous motility tracks were enlarged by selecting the track under the software's EDIT function to highlight the difference between the angles of adjacent points. Tracks displaying nonvigorous motility were classified as either slow or weakly motile (F and G, arrows). The images of these nonvigorous motility patterns include nearby vigorous tracks to illustrate the differences in track length.

little forward progress. Sperm tracks that could not be confidently assessed (overlapping tracks, tracks resulting from morphologically abnormal sperm or sperm that were adherent to the slide, or tracks that did not meet our strict criteria for each motility group) were excluded from the training set to reduce noise and observer bias.

A total of 2817 tracks from 18 individuals were used in the training set, with 1120 tracks classified as progressive, 173 as intermediate, 308 as hyperactivated, 746 as slow, and 470 as weakly motile. The hyperactivated class included star-spin, transitional, and asymmetric motility patterns [16, 34, 43], as shown in Figure 2C–E. The distribution and median values for the kinetic parameters of sperm in each group are displayed as boxplots in Figure 3, illustrating CASA parameter variation within and between CASAnova classes. Mean kinematic values $\pm$ SEM for each motility group are shown in Supplementary Table S1 to demonstrate differences between vigorous (progressive, intermediate, hyperactivated) and nonvigorous (slow, weakly motile) motility groups. In general, the means and medians are very similar.

Training of human CASAnova model and software development

Kinematic parameters were used to construct multidimensional scatter plots to show the distribution of sperm in each of the five motility groups (Figure 4A). Human sperm tracks clustered largely according to their visual classification. Briefly, weakly motile tracks (cyan) displayed the least robust motility and lowest velocities of all tracks. Slow tracks (black) clustered between progressive (pink) and weakly motile tracks, demonstrating the reduction in velocity that delineates vigorous versus nonvigorous motility. The clusters of progressive and hyperactivated (blue) sperm tracks were separated by the cluster of intermediate tracks (green), suggesting that the intermediate patterns may constitute a transitional state between progressive and hyperactivated motility. The distinct spatial clustering of human sperm motility patterns according to their visual classification indicates these patterns are amenable to mathematical separation using multiclass SVM algorithms.

Based on the independent kinematic parameters (VAP, VSL, VCL, ALH, and BCF) for each sperm track in the training set, we used the MatLab's LIBSVM function to identify a set of four linear equations that partition each motility group according to the

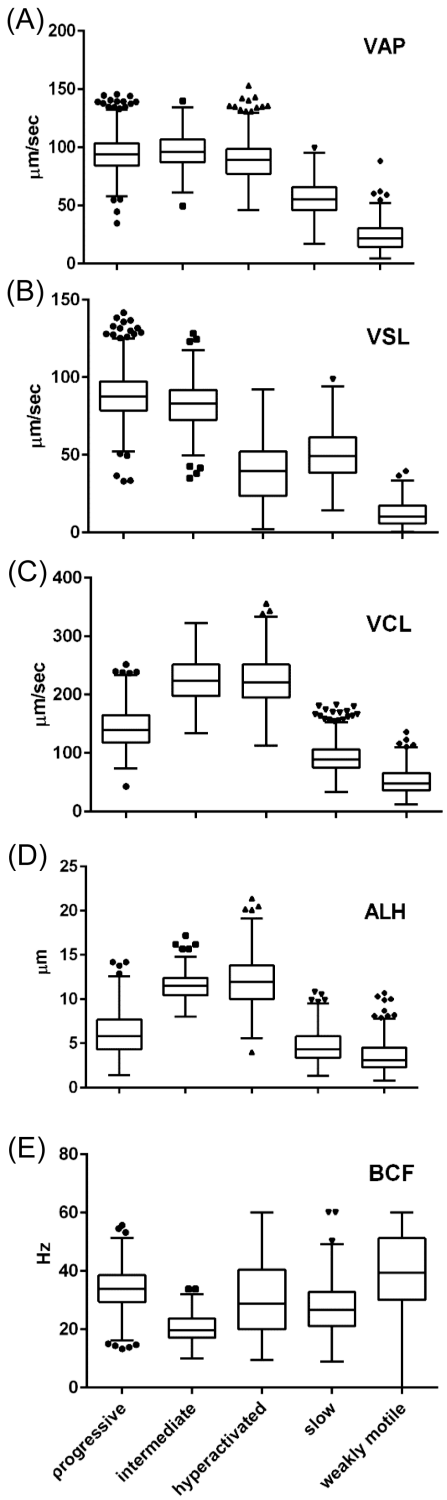

Figure 3. Medians and distributions of kinematic parameters for tracks used in training of human CASAnova model. Kinematic parameters of VAP (A), VSL (B), VCL (C), ALH (D), and BCF (E) for each CASAnova classification are shown as Tukey box plots. Each box displays the limits of the interquartile range (IQR) with horizontal lines at the median, 25th and 75th percentiles. Whiskers indicate the highest data point within 1.5 × IQR of the upper quartile and the lowest data point with 1.5 × IQR of the lower quartile, with outliers shown as symbols above and below the whiskers.

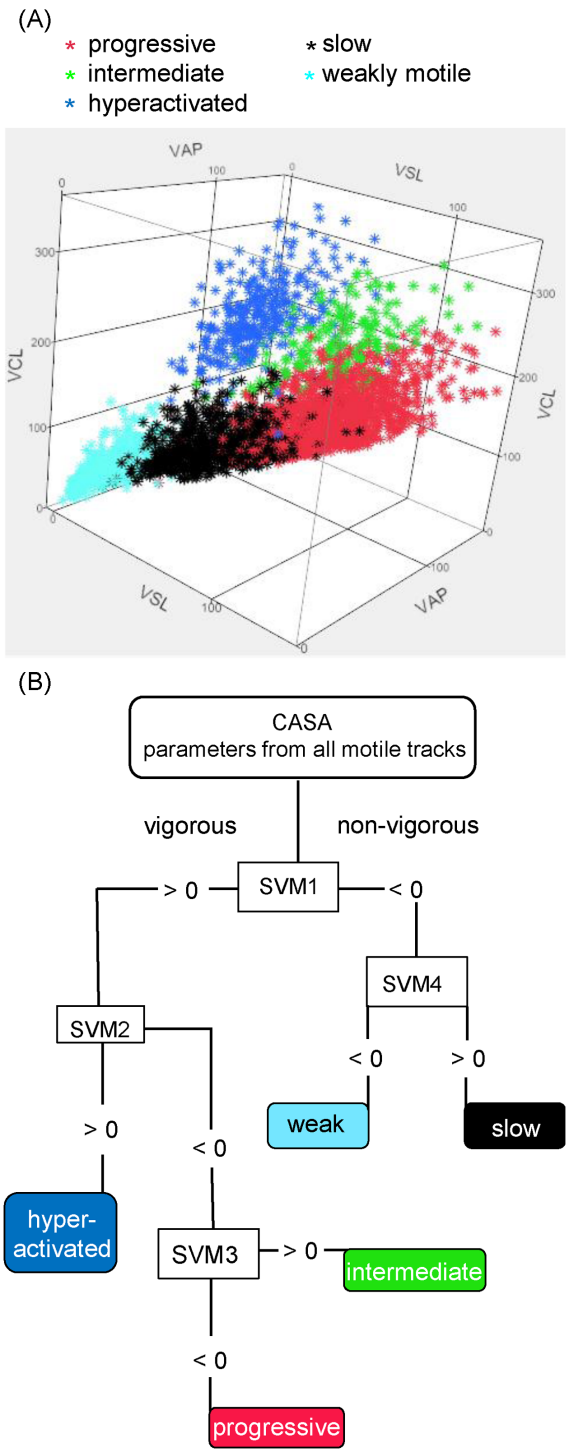

Figure 4. Multidimensional clustering of visually classified sperm tracks and generation of a multiclass SVM model. Sperm incubated for 3 h in HTF complete medium were visually classified according to motility pattern to generate a training set for human CASAnova. Tracks were then plotted as a function of their independent kinematic parameters (VAP, VSL, VCL, ALH, and BCF) in a multidimensional scatter plot (A). VAP, VSL, and VCL axes are shown in this plot. Progessive sperm are represented in the bottom right cluster. Intermediate sperm cluster in the center-right of the plot while hyperactivated sperm are clustered in the top center portion of the plot. Slow sperm and weakly motile sperm are clustered in the bottom center and bottom left of the plot, respectively. (B) Decision tree model demonstrating how SVM equations are sequentially applied to CASA track parameters to identify sperm motility patterns.

Table 1. Performance measures of the CASAnova model.

	Progressive (%)	Intermediate (%)	Hyperactivated (%)	Slow (%)	Weakly motile (%)
Precision	90.19	89.87	95.30	85.83	92.02
Sensitivity	92.77	82.08	92.21	82.84	95.74
Specificity	93.34	99.39	99.44	95.07	98.34

Performance measures for each class were calculated from the confusion matrix shown in Supplementary Table S3 using these standard formulas:

Precision (positive predictive value) = true positives/true positives + false positives.

Sensitivity (true positive rate) = true positives/true positives + false negatives.

Specificity (true negative rate) = true negatives/true negatives + false positives.

decision tree shown in Figure 4B. This was done by randomly dividing the training set into five groups, where four groups were used as a training set of data and the remaining group was used to test the accuracy of the equations. This process was repeated 100 times, and the best set of SVM equations was identified. The four SVM equations (Supplementary Table S2) in the set include the five independent CASA parameters structured as follows: $\text{SVM} = C_1(\text{VAP}) + C_2(\text{VSL}) + C_3(\text{VCL}) + C_4(\text{ALH}) + C_5(\text{BCF}) + b$, where the coefficient C_i of each parameter reflects its weight in determining the outcome of the equation, and b is an equation-specific constant value. The equations are applied sequentially, as depicted in Figure 4B. First, the model takes the CASA parameters for each track and inputs them into a binary SVM. If the product of the equation is greater than or equal to zero, the track is classified as vigorous. If the result is less than zero, the track is classified as nonvigorous. After defining two groups with the initial equation, the process is performed with additional equations to classify vigorous sperm as progressive, intermediate, or hyperactivated, and nonvigorous sperm as slow or weakly motile. Performance measures (Table 1) were calculated from a confusion matrix, specifying the number of correct and incorrect CASAnova classification for each of the five motility groups (Supplementary Table S3). The overall accuracy of this model is 89.92%, with individual precisions ranging from 85.83% for sperm classified as slow to 95.30% for sperm classified as hyperactivated (Table 1). Sensitivity and specificity measures for all five classes are also provided in Table 1.

We generated human sperm-specific CASAnova software that incorporates these four SVM equations to automatically classify individual human sperm tracks. This program utilizes CASA-generated track files containing the independent CASA parameters for each motile track. CASAnova applies the SVM equations to individual sperm tracks and generates a summary showing the total number of sperm that were classified into each motility group and the percentage of motile tracks in each group. The CASAnova software was developed into a web-based platform and is available for use at http://www.uncnri.org/casanova. The original software for mouse sperm is also available for use at this site.

Motility profiles throughout in vitro capacitation

To assess temporal changes in motility patterns during the in vitro capacitation of human sperm, we used our human CASAnova model to monitor motility at 1-h intervals throughout a 5-h time course (Figure 5). All motile sperm from the original 18 subjects and 8 additional subjects were included in this analysis. The average percentage of motile sperm was steady over this incubation period, remaining above 65% throughout the assay. At the initial time point (within 2 min of resuspension in HTF complete medium), sperm motility was equally divided between vigorous and nonvigorous patterns (49% vs 51%, respectively). Approximately 94% of the vigorous motility profiles were classified as progressive, with a mean of 2.6 ± 0.59% profiles exhibiting early hyperactivation. Within 1 h, the mean percentage of both intermediate and hyperactivated tracks increased, comprising ~15% of the motile population. Over the remainder of the time course, intermediate tracks increase slightly, with the mean reaching a maximum of 7.7 ± 1.5% by 5 h. Hyperactivated sperm tracks remained relatively constant, with a maximum mean of 9.6 ± 1.1% at 2 h. There was substantial variation between individuals in capacitation-associated changes in motility, with maximum levels of intermediate sperm varying between 1.89% and 29.1% and maximum hyperactivation varying between 5.3% and 27.3% over the time course. Concomitant with the increase in intermediate and hyperactivated motility patterns at 1 h, there was a reduction of ~8% in the mean percentage of slow sperm tracks. The mean percentages of the nonvigorous slow and weakly motile tracks remained relatively steady throughout the remainder of the capacitation period.

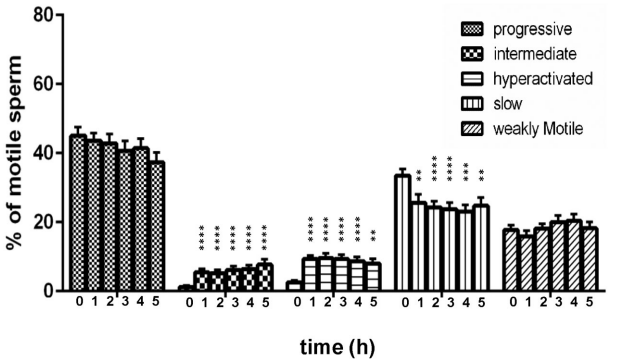

Figure 5. Motility profiles of capacitating human sperm. Motility was monitored at 1-h intervals by CASA. Independent kinematic parameters generated in these analyses were then used to classify all motile sperm using the human CASAnova program. Bars represent the mean ± SEM of motile tracks from 26 individuals. Differences between motility groups at corresponding time points were determined by one-way ANOVA after arcsine transformation of percentages followed by Dunnett's post test for multiple comparisons with time 0 as a control. * $P < 0.05$, ** $P < 0.01$, *** $P < 0.001$, **** $P < 0.0001$.

In a separate experiment, we conducted repeated CASA and CASAnova analyses on 10 aliquots from the same sperm sample after incubation for 3 h in HTF complete medium. The mean percentage of motile sperm in these aliquots was 85.9 ± 0.4% (with a median of 86%) and the motility profiles identified with CASAnova were quite reproducible in all 10 aliquots, with standard errors <1.2% (Supplementary Table S3).

Motility profiles of human sperm incubated under noncapacitating conditions

To determine if CASAnova is sufficiently sensitive to detect changes in motility when capacitation-associated signaling pathways are inhibited, we directly compared motility in eight sperm samples that were split and incubated for 5 h in either capacitating HTF medium or noncapacitating mHTF (Figure 6). While the mean percentage of motile sperm was maintained at comparable levels near 60% in either medium (Figure 6A), we did observe shifts in motility profiles between capacitating and noncapacitating media. In the absence of sufficient capacitation signals, the mean percentage of slow sperm exceeded 46% of the total motile population throughout the incubation period, significantly higher than the levels of approximately

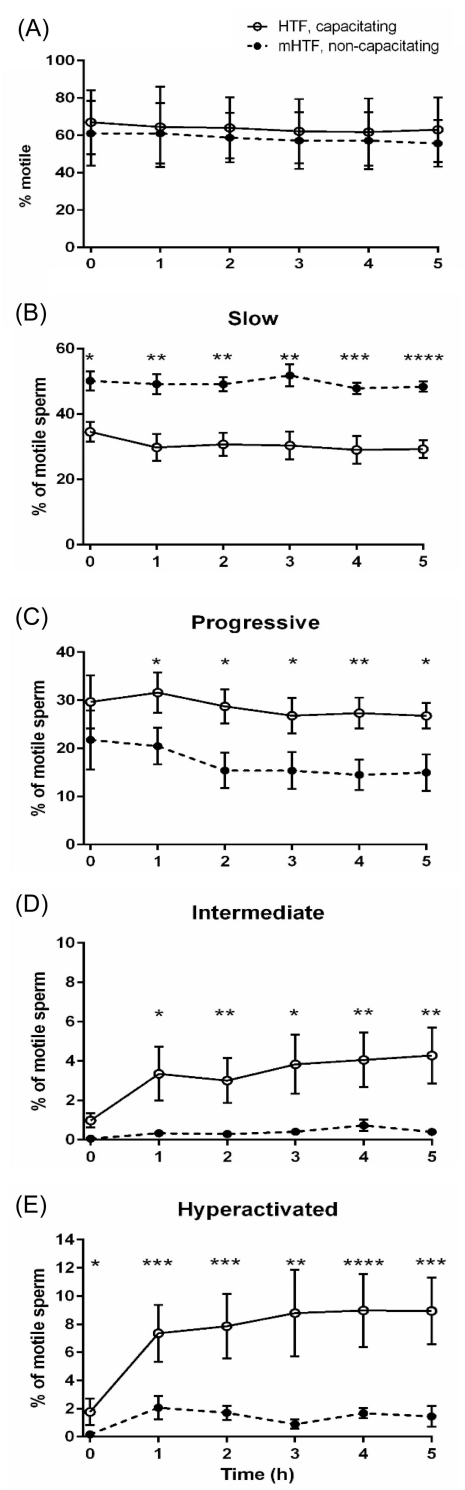

Figure 6. Vigorous motility patterns are reduced significantly when human sperm are incubated under noncapacitating conditions. Sperm samples from eight individuals were split and incubated for 5 h in either HTF (capacitating, solid lines) or mHTF (noncapacitating, dashed lines) medium. Aliquots were assessed for motility at 1-h intervals, and motility profiles were determined by CASAnova. Bars represent the mean ± SEM of motile tracks. Differences between motility groups at corresponding time points were determined by two-tailed unpaired t-test after arcsine transformation of percentages. * $P < 0.05$, ** $P < 0.01$, *** $P < 0.001$, **** $P < 0.0001$.

30% slow sperm when incubated in capacitating medium (Figure 6B). This increase in slow motility patterns was accompanied by decreases in all vigorous motility groups, including progressive sperm motility (Figure 6C). Both intermediate and hyperactivated motility were greatly reduced in noncapacitating sperm, although a small percentage (mean = 2.07 ± 0.83% at 1 h) of sperm were hyperactivated (Figure 6D and E). The mean percentages of weakly motile sperm were comparable in both media, remaining ~31% throughout the incubation.

Comparison of CASAnova vs kinematic gating approaches for identifying hyperactivation

Tracks are typically identified as hyperactivated based on kinematic gates, most frequently tracks with VCL ≥ 150 μm/s, LIN ≤ 50%, and ALH ≥ 7 μm when analyzed at 60 Hz [17]. Using these gates, we found that many of the tracks identified as hyperactivated (cyan or green tracks in Figure 1) were predominantly linear (tracks with asterisks in Figure 1) and distinct from typical hyperactivated tracks identified by visual inspection [16, 34, 43]. Tracks identified as hyperactivated with these gates were frequently observed at the initial time point (Figure 1A), prior to in vitro capacitation. Consequently, the gating approach appeared to overestimate the percentage of hyperactivated sperm. To evaluate CASAnova's ability to detect hyperactivation in human sperm, we compared the percentages of hyperactivated tracks identified with three methods: visual counting by a skilled observer not involved in the training of the model, kinematic gates (VCL ≥ 150 μm/s, LIN ≤ 50%, and ALH ≥ 7 μm), and CASAnova. Sperm samples from 13 individuals were selected randomly, and a set CASA tracks was collected for each sample immediately after resuspension in HTF complete medium (0 h, 274.4 ± 55.3 sperm tracks per sample, Figure 7A) and after 3 h incubation in capacitating medium (271.3 ± 47.2 sperm tracks per sample, Figure 7B). The percentage of hyperactivated tracks in each set was assessed using these three methods. At time 0 h, visual estimates of hyperactivation ranged from 0% to 10.2%, with a mean of 2.82 ± 0.83%. The percentages of hyperactivated sperm identified by kinematic gating at 0 h were consistently and significantly higher relative to visual analyses, with a mean of 9.54 ± 2.87% ($P < 0.05$ relative to visual assessment). CASAnova, by contrast, calculated a mean of 3.62 ± 1.06% hyperactivated sperm at this initial time point. After incubation in HTF complete medium for 3 h, the mean percentage of hyperactivated sperm was 8.74 ± 1.79% determined by visual inspection and 8.87 ± 1.86% by CASAnova (Figure 6B). Kinematic gates calculated the percentage of hyperactivated sperm as 23.31 ± 3.28% at this time point ($P < 0.0001$ vs. visual calculations). The gating estimates of hyperactivated sperm were higher than the combined percentages of hyperactivated and intermediate motility patterns identified by CASAnova at both 0 (2.78 ± 1.4%) and 3 h (10.6 ± 2.78%). Therefore, the inclusion of an intermediate motility pattern in the CASAnova method does not explain the difference in the percentage of hyperactivated sperm calculated with this method and kinematic gating.

To better understand the differences between sperm classified as hyperactivated using kinematic gates or CASAnova, all the tracks identified as hyperactivated with gates in Figure 7A and B were assessed to determine how these tracks were classified by CASAnova (Figure 7C and D). At 0 h, CASAnova classified 53.27 ± 8.54% of the gated tracks as progressive and 12.67 ± 4.03% as intermediate, with only 26 ± 8.1% classified as hyperactivated (Figure 7C). The lower percentages of hyperactivated motility identified by CASAnova

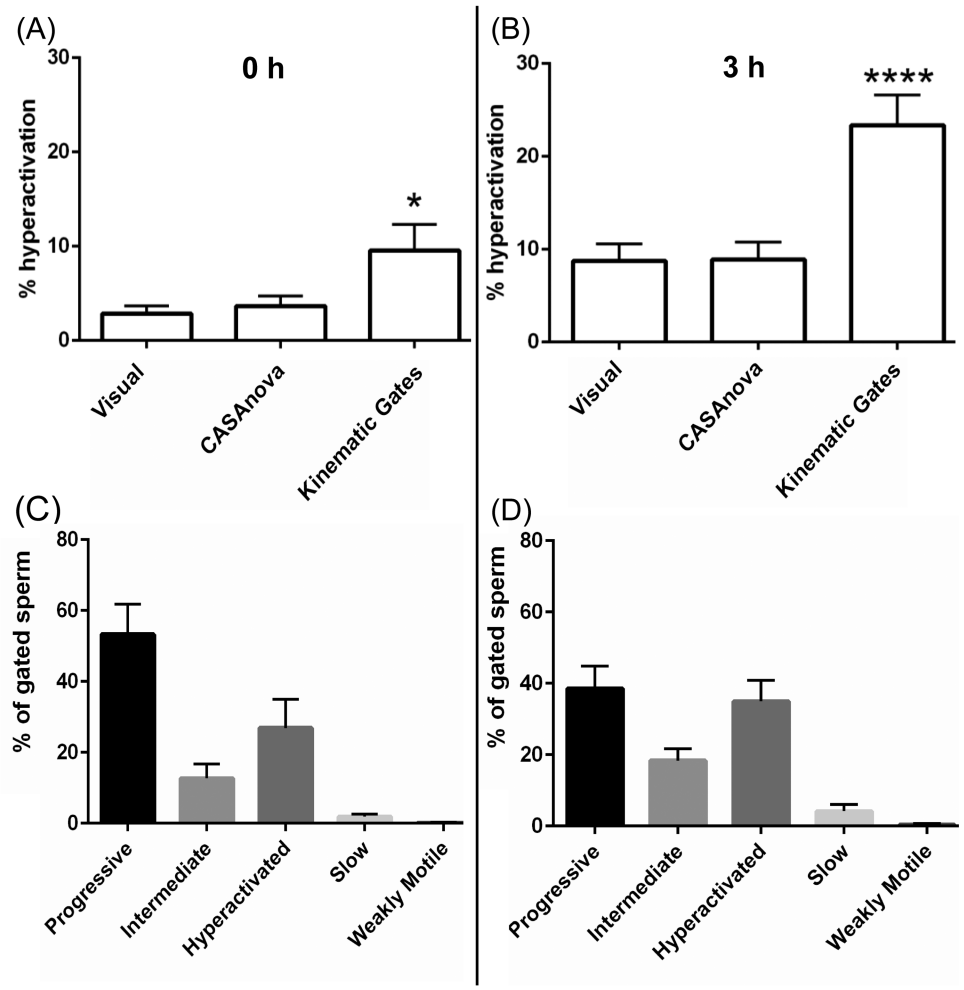

Figure 7. Comparison of visual counting, CASAnova, and kinematic gates to identify hyperactivated sperm. Sperm motility tracks from 13 individuals were assessed visually to determine the percentage of hyperactivated sperm at 0 h (A) and after 3 h (B) incubation in capacitating medium. Hyperactivation levels identified via CASAnova and kinematic gates were compared to visual assessments. (C and D) Sperm identified as hyperactivated using kinematic gates (VCL $\geq$ 150 μm/s, LIN $\leq$ 50%, and ALH $\geq$ 7 μm) were obtained using the SORT function on the CASA software. Kinematic parameters of these gated sperm were analyzed to determine the distribution of their motility patterns as identified by CASAnova. Data are represented as mean $\pm$ SEM. Differences between visual and other estimates of hyperactivation were determined by one-way ANOVA followed by Dunnett's post test for multiple comparisons. $^{*}P < 0.05$, $^{****}P < 0.0001$.

better reflect the expected physiological state of sperm at the initial time point, since the onset of robust hyperactivation only occurs after time spent in capacitation medium [47, 48]. The CASAnova classification of gated tracks after 3 h in capacitating medium was also assessed (Figure 7D). As expected, a higher percentage (35 $\pm$ 5.8%) of these tracks was identified as hyperactivated. Most of the remaining gated tracks were distributed between progressive and intermediate motility groups (32.6 $\pm$ 6.34% and 18.4 $\pm$ 3.29%, respectively).

Discussion

This study employed a standard supervised machine learning method to develop the first detailed CASA guidelines for classifying all motility patterns of human sperm that occur during in vitro capacitation after processing to remove seminal plasma. Machine learning methods are becoming increasingly important computational tools in science and medicine [49, 50]. The SVM-based decision tree method performs well as a classification algorithm because it determines a set of optimal hyperplanes that separate classes [51, 52]. These unique hyperplanes are optimal in the sense that they identify the largest possible margin between individuals in different classes. There is no subjectivity in selecting the hyperplanes since each is computed as a straightforward linear optimization.

The initial step in developing our CASAnova model was the preparation of a training set of visually classified sperm tracks. To minimize subjectivity, we employed strict criteria for the identification of three classes of vigorous motility (progressive, intermediate, and hyperactivated) and two classes of nonvigorous motility (slow and weakly motile). Our criteria were based on published examples of human sperm tracks and on similarities with mouse sperm tracks used in the training set for our original CASAnova model [23]. Only CASA tracks that met our stringent criteria and were consistently classified by at least two observers were included in our training set of 2817 human sperm tracks. Multidimensional scatter plots of velocity parameters (Figure 4A) confirmed that our classifica-

tion criteria distinguish five distinct motility patterns. We then used the SVM approach to develop the CASAnova model based on the independent kinematic parameters of sperm tracks in our training set. CASAnova for human sperm includes four SVM equations (Supplementary Table S2), with each equation defining a hyperplane between two classes of sperm motility. This model was optimized by conducting 100 independent iterations with our training set of CASA tracks. The final model performed with an overall accuracy of 89.9%, with individual class precisions between 85.8% and 95.3%.

We used CASAnova to classify all motile sperm in samples from 26 individuals at 1-h intervals throughout a 5-h in vitro capacitation period (Figure 5). More than 26 000 motile sperm were automatically classified in this experiment, enabling a rapid and quantitative analysis of changes in human sperm motility that occur during capacitation. Comparable percentages of vigorous and nonvigorous motility were maintained throughout the 5-h incubation period. In similar analyses of mouse sperm, vigorous motility was ~80% immediately after isolation, but declined to ~50% within 90 min [23]. Approximately 20% of human sperm were identified as weakly motile throughout the incubation period compared to ~10% of mouse sperm, perhaps reflecting greater heterogeneity of sperm quality in humans [53]. In both species, progressive patterns were predominant at the initial time point, with subsequent increases in intermediate and hyperactivated motility patterns apparent after capacitation for 1 h. Additional experiments confirmed the reproducibility of the CASAnova classification (Supplementary Table S4) and demonstrated that both intermediate and hyperactivated motility patterns are dependent upon incubation under capacitating conditions (Figure 6).

CASA settings used to classify human sperm motility patterns typically rely on gating methods and reflect recommendations in the WHO guidelines for semen analysis. The fourth edition of these guidelines [4] recommended classification of progressive motility as rapid ($\geq$25 μm/s) or slow ($<$25 μm/s and $>$5 μm/s), based on visual assessment with a standard microscope. Difficulties in assessing this distinction microscopically led to its elimination in the fifth edition [40]. Nevertheless, clinically important differences between rapid and slow sperm have been reported (reviewed in [54]), and CASA recommendations still suggest this distinction based on combinations of VAP, VSL, and STR criteria. An important goal of our CASAnova model was to identify distinct categories of motility and provide a single classification for each motile sperm in a population. Both published CASA analyses [55, 56] and our results indicate that washed human sperm with vigorous motility have VAP values that are significantly higher than the 25 μm/s cutoff recommended for identifying "rapid" sperm in semen samples [4]. The CASAnova model effectively distinguishes vigorous sperm (progressive, intermediate, and hyperactivated) with average VAP values near 90 μm/s from the nonvigorous categories of slow and weakly motile sperm with average VAP values of 55.6 and 23.6 μm/s, respectively (Figure 3 and Supplementary Table S1). The inclusion of nonvigorous motility groups in CASAnova permits more detailed analysis of heterogeneity in sperm motility patterns, which may prove useful for evaluating compounds that either enhance motility for assisted reproduction [57] or inhibit motility in applications such as reproductive toxicology [58, 59] or contraceptive development [60].

To assess the sensitivity of CASAnova in detecting capacitation-dependent changes in human sperm motility, we applied this method to sperm samples that were split and incubated under capacitating or noncapacitating conditions in parallel (Figure 6). In mice, the incubation of sperm in noncapacitating medium led to an inability of sperm to switch from predominantly progressive motility to other forms of vigorous motility [23]. As expected, intermediate and hyperactivated motility patterns were also nearly eliminated when human sperm were incubated under noncapacitating conditions. Unlike mouse sperm, however, human sperm motility was predominantly slow in the absence of bicarbonate, suggesting that capacitation-associated signals trigger a burst of activity that accelerates sperm velocity. This burst in progressive sperm motility in response to bicarbonate is rapid, as initial time points were typically completed within 2 min of dilution into capacitating medium. These results demonstrate that CASAnova is able to reflect changes in motility patterns during capacitation in association with perturbations in bicarbonate-dependent signaling pathways.

Like sperm from several mammalian species, hyperactivated human sperm display large amplitude flagellar waves causing side-to-side movement of the sperm head with reflex positions relative to the cell axis. We examined both progressive and hyperactivated tracks in studies that were instrumental in identifying characteristic features of human hyperactivation. These earlier studies visually classified sperm motility patterns based on video recordings of flagellar movement [11, 16, 61] and CASA tracks resulting from the consequent changes in sperm head position [34, 43, 62]. Bending in the proximal flagellum increases during hyperactivation, generating characteristic CASA tracks with reduced forward movement, large deviations from the average path, and marked angles between points as sperm change direction. Comparable examples of hyperactivated tracks from our CASA recordings are shown in Figure 2. In addition to track length and displacement from the average path, we examined angles between consecutive points in the track and assessed whether the majority were generally less than, equal to, or greater than 90°. In other studies, angular deviation of the head was also considered to be an important metric for determining if a track is hyperactivated [63, 64]. Sperm tracks identified as hyperactivated by CASAnova exhibited increase in VCL and ALH and decrease in VSL compared to progressive tracks (Figure 3 and Supplementary Table S1), confirming their expected similarities to published examples of hyperactivated tracks [16, 18, 34, 43, 44, 65].

In comparing the percentages of hyperactivated human sperm determined by visual assessment, kinematic gating, and CASAnova, we found that CASAnova more accurately reflected visual estimates of hyperactivation (Figure 7). The levels of hyperactivation assessed visually and by CASAnova are lower than those previously reported for human sperm [11, 17, 34]. Multiple factors may contribute to these differences, including variations in sperm processing and heterogeneity between individuals. Also, CASAnova provides a single classification for each motile sperm, unlike standard gates which may classify some tracks as both progressive and hyperactivated (cyan tracks in Figure 1). In this study, we found that many of the sperm tracks identified as hyperactivated using kinematic gates [17] displayed motility patterns identified as intermediate and progressive with CASAnova. Whether the intermediate group constitutes a subtype of hyperactivated motility is unknown, as they are visually distinguishable from transitional hyperactivated sperm (Figure 2) [23] but do not conform to the criteria defining progressive sperm patterns. Nevertheless, inclusion of the intermediate group does not fully explain differences in estimates of hyperactivation, since approximately 40% of sperm tracks designated hyperactivated using gates were identified as progressive with CASAnova. It is interesting to note that intermediate tracks typically exhibit high VCL and ALH values that are comparable to hyperactivated tracks, but have higher VSL values comparable to progressive tracks (Figure 3 and Supplementary Table S1).

Of the approximately 15% of couples affected by reproductive issues, approximately half are due to male factor infertility [66–68]. Up to one third of these cases are classified as idiopathic [69], suggesting that the current methods of assessing sperm function are not capable of detecting many causes of infertility. Since changes in sperm swimming patterns are intrinsically linked to the ability of sperm to fertilize the egg under normal conditions, alterations in these pathways are potential sources of male infertility that may escape notice using conventional sperm analysis. Studies focusing on the basic genetic, molecular, or pharmaceutical control of human sperm motility would benefit from a method enabling a more detailed analysis of all sperm in a population. The ability of CASAnova to assess multiple patterns of sperm motility in a robust, automated, and quantitative manner makes it an attractive option for these types of studies. Since CASAnova is now available for mouse and human sperm, we anticipate that this approach will be particularly useful in investigations aimed at translating knowledge gained in mouse models to enhance our understanding of pathways that regulate human sperm motility. In addition, development of the human CASAnova model offers a tool that may prove useful in the clinical assessment of idiopathic infertility.

Supplementary data

Supplementary data are available at *BIOLRE* online.

Supplementary Table S1. Average kinematic parameters (mean ± SEM) of tracks used in training of human CASAnova model.
Supplementary Table S2. Human CASAnova support vector machine (SVM) equations.
Supplementary Table S3. Confusion matrix for the CASAnova model.
Supplementary Table S4. Reproducibility of CASAnova classifications.

Acknowledgments

The authors wish to thank Tondra Blevins for her outstanding clinical and technical expertise in support of this work and Kathryn E Kirchoff for assistance with computing performance metrics for the CASAnova model.

Authors' contributions: SGG conceived the concept for this project and had primary responsibility for all aspects of data acquisition, data analysis, and manuscript preparation. AMS and SB performed visual classifications to generate the training set data, TRM performed experiments and interpreted results, and MMK assisted with approach and methodology. SW, C-YK, and LM performed computer methodologies and SJ designed the web application. SHZ participated in data analysis and manuscript preparation. DAO contributed to the experimental design, data analysis, and manuscript preparation.

Conflict of interest: The authors have declared that no conflict of interest exists.

References

1. Kwack SJ, Lee B. Comparative cytotoxicity and sperm motility using a computer-aided sperm analysis system (CASA) for isomers of phthalic acid, a common final metabolite of phthalates. *J Toxicol Environ Health A* 2015; **78**:1038–1050.
2. Tamburrino L, Marchiani S, Minetti F, Forti G, Muratori M, Baldi E. The CatSper calcium channel in human sperm: relation with motility and involvement in progesterone-induced acrosome reaction. *Hum Reprod* 2014; **29**:418–428.
3. SepúLveda L, Bussalleu E, Yeste M, Bonet S. Effect of Pseudomonas aeruginosa on sperm capacitation and protein phosphorylation of boar spermatozoa. *Theriogenology* 2016; **85**:1421–1431.
4. World Health Organization. *WHO Laboratory Manual for the Examination of Human Semen and Sperm-Cervical Mucus Interaction*. Cambridge, UK; New York, NY: Published on behalf of the World Health Organization [by] Cambridge University Press; 1999.
5. Yanagimachi R. Mammalian fertilization. In: Knobil E, Neill J (eds.) *The Physiology of Reproduction*. New York: Raven Press; 1994: 189–317.
6. Suarez SS. Control of hyperactivation in sperm. *Hum Reprod Update* 2008; **14**:647–657.
7. Qi H, Moran MM, Navarro B, Chong JA, Krapivinsky G, Krapivinsky L, Kirichok Y, Ramsey IS, Quill TA, Clapham DE. All four CatSper ion channel proteins are required for male fertility and sperm cell hyperactivated motility. *P Natl Acad Sci USA* 2007; **104**:1219–1223.
8. Olds-Clarke P. Sperm from tw32/+ mice: capacitation is normal, but hyperactivation is premature and nonhyperactivated sperm are slow. *Dev Biol* 1989; **131**:475–482.
9. Ho K, Wolff CA, Suarez SS. CatSper-null mutant spermatozoa are unable to ascend beyond the oviductal reservoir. *Reprod Fertil Dev* 2009; **21**:345–350.
10. Ren D, Xia J. Calcium signaling through CatSper channels in mammalian fertilization. *Physiology* 2010; **25**:165–175.
11. Burkman LJ. Characterization of hyperactivated motility by human spermatozoa during capacitation: comparison of fertile and oligozoospermic sperm populations. *Arch Androl* 1984; **13**:153–165.
12. Munire M, Shimizu Y, Sakata Y, Minaguchi R, Aso T. Impaired hyperactivation of human sperm in patients with infertility. *J Med Dent Sci* 2004; **51**:99–104.
13. Sukcharoen N, Keith J, Irvine DS, Aitken RJ. Definition of the optimal criteria for identifying hyperactivated human spermatozoa at 25 Hz using in-vitro fertilization as a functional end-point. *Hum Reprod* 1995; **10**:2928–2937.
14. Alasmari W, Barratt CLR, Publicover SJ, Whalley KM, Foster E, Kay V, Martins Da Silva S, Oxenham SK. The clinical significance of calcium-signalling pathways mediating human sperm hyperactivation. *Hum Reprod* 2013; **28**:866–876.
15. Williams HL, Mansell S, Alasmari W, Brown SG, Wilson SM, Sutton KA, Miller MR, Lishko PV, Barratt CL, Publicover SJ, Martins da Silva S. Specific loss of CatSper function is sufficient to compromise fertilizing capacity of human spermatozoa. *Hum Reprod* 2015; **30**:2737–2746.
16. Mortimer ST, Mortimer D. Kinematics of human spermatozoa incubated under capacitating conditions. *J Androl* 1990; **11**:195–203.
17. Mortimer ST, Swan MA, Mortimer D. Effect of seminal plasma on capacitation and hyperactivation in human spermatozoa. *Hum Reprod* 1998; **13**:2139–2146.
18. Mortimer ST. The development of smoothing-independent kinematic measures of capacitating human sperm movement. *Hum Reprod* 1999; **14**:986–996.
19. Chantler E, Abraham-Peskir J, Roberts C. Consistent presence of two normally distributed sperm subpopulations within normozoospermic human semen: a kinematic study. *Int J Androl* 2004; **27**:350–359.
20. Li C-Y, Jiang L-Y, Chen W-Y, Li K, Sheng H-Q, Ni Y, Lu J-X, Xu W-X, Zhang S-Y, Shi Q-X. CFTR is essential for sperm fertilizing capacity and is correlated with sperm quality in humans. *Hum Reprod* 2010; **25**:317–327.
21. Mortimer D, Mortimer ST. Computer-aided sperm analysis (CASA) of sperm motility and hyperactivation. *Methods Mol Biol* 2013; **927**:77–87.
22. Li K, Xue Y, Chen A, Jiang Y, Xie H, Shi Q, Zhang S, Ni Y, Zhang M. Heat shock protein 90 has roles in intracellular calcium homeostasis, protein tyrosine phosphorylation regulation, and progesterone-responsive sperm function in human sperm. *PLoS One* 2014; **9**:e115841.
23. Goodson SG, Zhang Z, Tsuruta JK, Wang W, O'brien DA. Classification of mouse sperm motility patterns using an automated multiclass support vector machines modelc *Biol Reprod* 2011; **84**:1207–1215.
24. Bennett KP, Blue JA. A support vector machine approach to decision trees. *IEEE World Cong Comput Intell* 1998; **3**:2396–2401.

25. Goodson SG, Qiu Y, Sutton KA, Xie G, Jia W, O'brien DA. Metabolic substrates exhibit differential effects on functional parameters of mouse sperm capacitation. *Biol Reprod* 2012; **87**:75.
26. Westmuckett AD, Nguyen EB, Herlea-Pana OM, Alvau A, Salicioni AM, Moore KL. Impaired sperm maturation in RNASE9 knockout mice. *Biol Reprod* 2014; **90**:120.
27. Navarrete FA, Garcia-Vazquez FA, Alvau A, Escoffier J, Krapf D, Sanchez-Cardenas C, Salicioni AM, Darszon A, Visconti PE. Biphasic role of calcium in mouse sperm capacitation signaling pathways. *J Cell Physiol* 2015; **230**:1758–1769.
28. Huang Z, Danshina PV, Mohr K, Qu W, Goodson SG, O'Connell TM, O'Brien DA. Sperm function, protein phosphorylation, and metabolism differ in mice lacking successive sperm-specific glycolytic enzymes. *Biol Reprod* 2017; doi: 10.1093/biolre/iox103.
29. Odet F, Pan W, Bell TA, Goodson SG, Stevans AM, Yun Z, Aylor DL, Kao C, Mcmillan L, De Villena FP, O'Brien DA. The founder strains of the collaborative cross express a complex combination of advantageous and deleterious traits for male reproduction. *G3 (Bethesda)* 2015; **5**(12):2671–2683.
30. Shorter JR, Odet F, Aylor DL, Pan W, Kao C, Fu C, Morgan AP, Greenstein S, Bell TA, Stevans AM, Feathers RW, Patel S et al. Male infertility is responsible for nearly half of the extinction observed in the mouse collaborative cross. *Genetics* 2017; **206**:557–572.
31. Gray JE, Starmer J, Lin VS, Dickinson BC, Magnuson T. Mitochondrial hydrogen peroxide and defective cholesterol efflux prevent in vitro fertilization by cryopreserved inbred mouse sperm. *Biol Reprod* 2013; **89**:17.
32. Navarrete FA, Alvau A, Lee HC, Levin LR, Buck J, Leon PM, Santi CM, Krapf D, Mager J, Fissore RA, Salicioni AM, Darszon A et al. Transient exposure to calcium ionophore enables *in vitro* fertilization in sterile mouse models. *Sci Rep* 2016; **6**:33589. doi: 10.1038/srep33589.
33. Liu DY, Clarke GN, Baker HW. Relationship between sperm motility assessed with the Hamilton-Thorn motility analyzer and fertilization rates in vitro. *J Androl* 1991; **12**:231–239.
34. Robertson L, Wolf DP, Tash JS. Temporal changes in motility parameters related to acrosomal status: identification and characterization of populations of hyperactivated human sperm. *Biol Reprod* 1988; **39**:797–805.
35. Donnelly ET, Lewis SEM, Mcnally JA, Thompson W. In vitro fertilization and pregnancy rates: the influence of sperm motility and morphology on IVF outcome. *Fertil Steril* 1998; **70**:305–314.
36. Visconti PE, Bailey JL, Moore GD, Pan D, Olds-Clarke P, Kopf GS. Capacitation of mouse spermatozoa. I. Correlation between the capacitation state and protein tyrosine phosphorylation. *Development* 1995; **121**:1129–1137.
37. Osheroff JE. Regulation of human sperm capacitation by a cholesterol efflux-stimulated signal transduction pathway leading to protein kinase A-mediated up-regulation of protein tyrosine phosphorylation. *Mol Hum Reprod* 1999; **5**:1017–1026.
38. Makler A, Stoller J, Makler-Shiran E. Dynamic aspects concerned with the mechanism of separating motile sperm from nonmotile sperm, leukocytes, and debris with the use of highdensity Percoll gradients. *Fertil Steril* 1998; **70**:961–966.
39. Tamburrino L, Marchiani S, Vicini E, Muciaccia B, Cambi M, Pellegrini S, Forti G, Muratori M, Baldi E. Quantification of CatSper1 expression in human spermatozoa and relation to functional parameters. *Hum Reprod* 2015; **30**:1532–1544.
40. World Health Organization. *WHO Laboratory Manual for the Examination and Processing of Human Semen*. Geneva: World Health Organization; 2010.
41. Quinn P, Kerin JF, Warnes GM. Improved pregnancy rate in human in vitro fertilization with the use of a medium based on the composition of human tubal fluid. *Fertil Steril* 1985; **44**:493–498.
42. Byers SL, Payson SJ, Taft RA. Performance of ten inbred mouse strains following assisted reproductive technologies (ARTs). *Theriogenology* 2006; **65**:1716–1726.
43. Burkman LJ. Discrimination between nonhyperactivated and classical hyperactivated motility patterns in human spermatozoa using computerized analysis. *Fertil Steril* 1991; **55**:363–371.
44. Mortimer ST. CASA–practical aspects. *J Androl* 2000; **21**:515–524.
45. Devijver PA, Kittler J. *Pattern Recognition: A Statistical Approach*. London, G.B.: Prentice-Hall; 1982.
46. Sokolova M, Lapalme G. A systematic analysis of performance measures for classification tasks. *Inform Process Manage* 2009; **45**:427–437.
47. Kay V. Hyperactivated motility of human spermatozoa: a review of physiological function and application in assisted reproduction. *Hum Reprod Update* 1998; **4**:776–786.
48. Visconti PE, Westbrook VA, Chertihin O, Demarco I, Sleight S, Diekman AB. Novel signaling pathways involved in sperm acquisition of fertilizing capacity. *J Reprod Immunol* 2002; **53**:133–150.
49. Jordan MI, Mitchell TM. Machine learning: trends, perspectives, and prospects. *Science* 2015; **349**:255–260.
50. Deo RC. Machine learning in medicine. *Circulation* 2015; **132**:1920–1930.
51. Yang ZR. Biological applications of support vector machines. *Brief Bioinform* 2004; **5**:328–338.
52. Noble WS. What is a support vector machine? *Nat Biotechnol* 2006; **24**:1565–1567.
53. Mortimer D, Mortimer S, Horst GD. The future of computer-aided sperm analysis. *Asian J Androl* 2015; **17**:545–553.
54. Barratt CLR, Bjorndahl L, Menkveld R, Mortimer D. ESHRE special interest group for andrology basic semen analysis course: a continued focus on accuracy, quality, efficiency and clinical relevance. *Hum Reprod* 2011; **26**:3207–3212.
55. Mortimer ST, Swan MA. Andrology: Kinematics of capacitating human spermatozoa analysed at 60 Hz. *Hum Reprod* 1995; **10**:873–879.
56. Larsen L. Computer-assisted semen analysis parameters as predictors for fertility of men from the general population. *Hum Reprod* 2000; **15**:1562–1567.
57. Tardif S, Madamidola OA, Brown SG, Frame L, Lefievre L, Wyatt PG, Barratt CL, Martins Da Silva SJ. Clinically relevant enhancement of human sperm motility using compounds with reported phosphodiesterase inhibitor activity. *Hum Reprod* 2014; **29**:2123–2135.
58. Slott V. Optimization of the Hamilton-Thorn computerized sperm motility analysis system for use with rat spermatozoa in toxicological studies. *Fundam Appl Toxicol* 1993; **21**:298–307.
59. Mehrpour O, Karrari P, Zamani N, Tsatsakis AM, Abdollahi M. Occupational exposure to pesticides and consequences on male semen and fertility: a review. *Toxicol Lett* 2014; **230**:146–156.
60. Danshina PV, Qu W, Temple BR, Rojas RJ, Miley MJ, Machius M, Betts L, O'brien DA. Structural analyses to identify selective inhibitors of glyceraldehyde 3-phosphate dehydrogenase-S, a sperm-specific glycolytic enzyme. *Mol Hum Reprod* 2016; **22**:410–426.
61. Morales P, Overstreet JW, Katz DF. Changes in human sperm motion during capacitation in vitro. *Reproduction* 1988; **83**:119–128.
62. Mortimer ST, Swan MA. Variable kinematics of capacitating human spermatozoa. *Hum Reprod* 1995; **10**:3178–3182.
63. Davis RO, Overstreet JW, Asch RH, Ord T, Silber SJ. Movement characteristics of human epididymal sperm used for fertilization of human oocytes in vitro. *Fertil Steril* 1991; **56**:1128–1135.
64. Mazzilli F, Rossi T, Delfino M, Dondero F, Makler A. A new objective method for scoring human sperm hyperactivation based on head axis angle deviation. *Int J Androl* 2001; **24**:189–196.
65. Mortimer S. A critical review of the physiological importance and analysis of sperm movement in mammals. *Hum Reprod Update* 1997; **3**:403–439.
66. Thonneau P, Marchand S, Tallec A, Ferial M, Ducot B, Lansac J, Lopes P, Tabaste J, Spira A. Incidence and main causes of infertility in a resident population (1 850 000) of three French regions (1988-1989). *Hum Reprod* 1991; **6**:811–816.
67. De Kretser DM, Baker HW. Infertility in men: recent advances and continuing controversies. *J Clin Endocrinol Metab* 1999; **84**:3443–3450.
68. Gnoth C. Definition and prevalence of subfertility and infertility. *Hum Reprod* 2005; **20**:1144–1147.
69. Gudeloglu A, Brahmbhatt JV, Parekattil SJ. Medical management of male infertility in the absence of a specific etiology. *Semin Reprod Med* 2014; **32**:313–318.